Journal of Statistical Physics, Vol. 65, Nos. 1/2, 1991

Repeller Structure in a Hierarchical Model. I. Topological Properties

R. Livi,[1,4] A. Politi,[2,4] and S. Ruffo[3,4]

Received December 20, 1990; final March 28, 1991

The repeller associated with the renormalization dynamics of the spectral problem of a hierarchical tight-binding Schrödinger equation is studied. Analysis of escaping regions and of stable and unstable manifolds provide complementary descriptions of the recurrent set, whose structure undergoes relevant changes when the growth rate R of the potential barriers is modified. The minimal region containing the repeller is determined and the mechanism originating a Cantor set structure along the unstable manifold is revealed. The repeller is continuous along the stable manifold for $R < 2$. Finally, we show the existence of a pointlike component of the spectrum located at its upper extremum for $R < 1$ and we present the associated wavefunctions.

KEY WORDS: Strange repellers; localization; Schrödinger operator; hierarchical structures; renormalization group.

1. INTRODUCTION

Fibonacci chains and hierarchical one-dimensional discrete Schrödinger operators have been introduced by various authors[1–6] as toy models for electronic conduction in etherostructures and superlattices where anomalous diffusive behaviors are expected.[7–9] These models have been extensively studied both numerically and analytically, showing many common interesting features. This is not surprising if one considers that the spectral problem is exactly solvable by renormalization group.[10–13] The general properties of these spectra can be summarized as follows:

[1] Dipartimento di Fisica, Università di Firenze, I-50125 Florence, Italy.
[2] Istituto Nazionale di Ottica, I-50125 Florence, Italy.
[3] Dipartimento di Chimica, Università della Basilicata, Potenza, Italy.
[4] Istituto Nazionale di Fisica Nucleare, Sezione di Firenze, Florence, Italy.

0022-4715/91/1000-0053$06.50/0

(i) The spectrum is a Cantor set.[12,13]

(ii) Scaling and measure-theoretic properties can be derived by renormalization group arguments.

(iii) A singular continuous component exists for some values of the parameters, where wavefunctions show a self-similar *critical* structure.[1,2,14]

Less is known on the aspects quoted in (ii) and (iii) for the hierarchical models. Some results were obtained about scaling laws of the density of states for specific components of the spectrum.[5] The self-similar properties of the wavefunctions have also been investigated numerically.[3,6,15] Anyway, a complete quantitative description of the scaling laws deriving from the renormalization dynamics was still lacking.

In this paper we make a first step toward such a quantitative description by analyzing the topological structure of the recurrent set associated with the renormalization group transformation. This is done by determining the escaping regions and the invariant manifolds. We find that the recurrent set is unstable, i.e., a repeller, continuous along its stable manifold in a suitable parameter range.

In Section 2 we define the model and briefly review the known results. In the first part of Section 3 we discuss the structure of the repeller by characterizing its complement: the regions which escape to infinity. In the second part we study the structure of the repeller along the stable manifold. In Section 4 we study the existence of localized states, connecting them with the intersection of the stable manifold of suitable fixed points. Section 5 is devoted to some concluding remarks.

Metric and multifractal properties will be treated in Part II.[16]

2. THE MODEL

The discrete one-dimensional Schrödinger operator H, first introduced in ref. 5, is defined as follows:

$$(H\psi)(i) = -[\psi(i+1) - 2\psi(i) + \psi(i-1)] + V(i)\,\psi(i) \tag{2.1}$$

where

$$V(i) = \lambda f(\mathrm{ord}(i)) \tag{2.2}$$

Here i labels the lattice sites, λ is a real parameter representing the strength of the potential, f is a real-valued function, and $\mathrm{ord}(i)$ is the largest nonnegative integer j such that 2^j is a divisor of i. In order to guarantee a

simple form of the renormalization transformation, f has been defined as follows:

$$f(j) = \frac{R^j - 1}{R - 1} \tag{2.3}$$

where R is chosen to be a positive real parameter. It has been shown that the semi-infinite chain spectral problem is equivalent to the doubly infinite one, if the potential in the origin is defined as follows[12]:

$$V(0) = \lambda \lim_{j \to \infty} f(j) = \begin{cases} \lambda/(1-R), & R < 1 \\ \infty, & R \geqslant 1 \end{cases}$$

The solution of the eigenvalue problem for the operator defined in (1.1), $H\psi(i) = E\psi(i)$, can be approached by applying a renormalization group transformation based on a decimation technique.[5],[5] For the potential given in (2.2) and (2.3) this procedure leads to the recursive relations

$$\begin{aligned} x_{n+1} &= 2 - x_n^2 + x_n y_n \\ y_{n+1} &= -R x_n y_n \end{aligned} \tag{2.4}$$

with initial conditions $x_0 = E - 2$ and $y_0 = \lambda$, where x_{n+1} and y_{n+1} represent the renormalized energy and potential strength, respectively (see ref. 5 for details).

Equation (2.4) has three fixed points in the (x, y) plane, namely

$$\begin{aligned} F1 &= (-2, 0) \\ F2 &= (1, 0) \\ F3 &= (-1/R, (2R^2 + R - 1)/R) \end{aligned} \tag{2.5}$$

Stability analysis shows that $F1$ and $F2$ possess an unstable manifold along the x axis and a stable (unstable) manifold transverse to the x axis for $R < 1/2$ ($R > 1/2$) and $R < 1$ ($R > 1$), respectively. The fixed point $F3$ is an unstable focus up to $R = 1/2$, where it coincides with the fixed point $F1$, then becoming a saddle for $R > 1/2$. A complete study of the dynamics (2.4) needs first the characterization of its recurrent set. As usual, when dealing with renormalization group transformations, we expect the presence of a repeller which can be identified as the intersection of a stable and an unstable manifold. This is indeed the case, as it will become clear in the following sections.

[5] This method has been shown in ref. 12 to be equivalent to the determination of the recursive relations for the traces of the transfer matrices.

3. ESCAPING REGIONS AND MANIFOLDS

As a first goal, we want to study the geometrical features of the set of points recurrent under map (2.4). As this turns out to be an unstable set, it is by definition a repeller. Two main families of strange repellers have been so far identified: (a) Cartesian products of two Cantor sets (as it is the case of the renormalization group transformation associated with Fibonacci chains[1,2,10]) typical of invertible 2d maps, which occur when a Smale horseshoe is generated by the dynamics; (b) fully unstable repellers occurring in noninvertible maps like Julia sets which can be easily generated by iterating backward the map and choosing randomly the preimage.[17] In the case of map (2.4), we expect a "mixture" of the two cases, because, as, we will see in the following, the dynamics is not fully unstable and the map is noninvertible. In fact, the inverse of map (2.4) reads

$$\begin{aligned} x_{n-1} &= \pm(2 - x_n - y_n/R)^{1/2} \\ y_{n-1} &= -y_n/(Rx_{n-1}) \end{aligned} \tag{3.1}$$

A noninvertible map, which is often only approximately related to equations describing physical systems, is here a rigorous consequence of the renormalization group, which, being a semigroup, contains in a natural

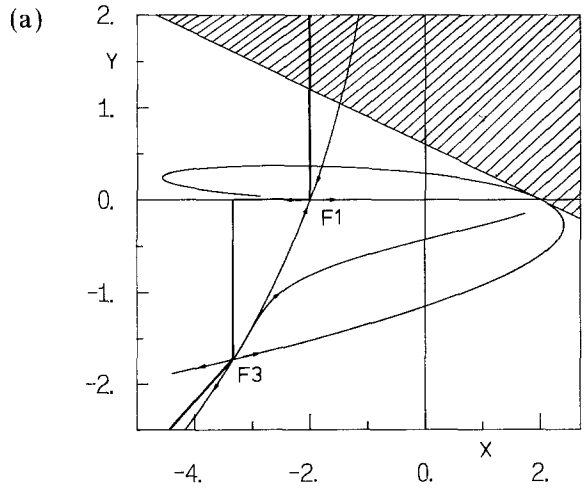

Fig. 1. Escaping region of map (2.4) for $R = 0.3$ (a), 0.7 (b), and 1.5 (c). The shaded triangles indicate the noninvertibility region. The piecewise straight lines represent the border of the first-order approximation L_0 of the escaping region. The remaining curves represent the invariant manifolds of the fixed points $F1$ and $F3$.

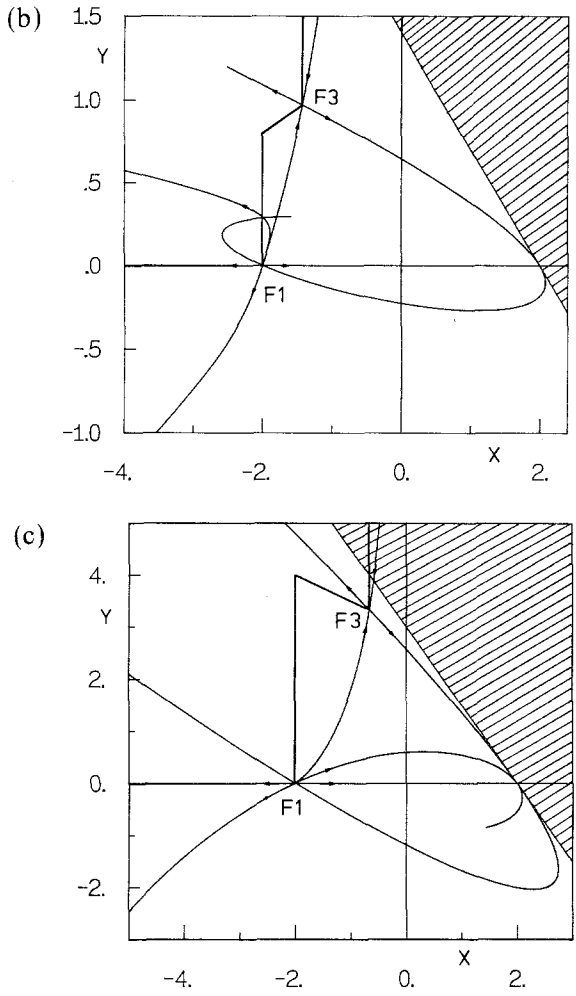

Fig. 1. (*Continued*)

way a preferred direction. It is easily seen that in the region (shaded in Fig. 1)

$$y > R(2-x) \tag{3.2}$$

no preimage exists, so that we cannot find points of the repeller there. In the remaining half-plain, instead, two preimages P_1 and P_2 exist, related by the symmetry operation $P_2 = S(P_1)$, where S is defined by

$$S(x, y) = (-x, -y) \tag{3.3}$$

Moreover, we observe that the x axis is left invariant by map (2.4) for any value of R, and the dynamics on it is the same as the one exhibited by the logistic map at the Ulam point. As a consequence, the interval on the x axis delimited by $F1$ and by $(2, 0)$ belongs to the repeller. The remaining nontrivial part of the repeller will be characterized by a standard procedure. The structure along the stable and unstable manifolds will be investigated looking for the regions which escape (either diverging to infinity, or converging to some attractor) backward and forward from the repeller, respectively. The repeller turns out to be the intersection of such manifolds. The analysis of escaping regions was already performed in ref. 12 to identify the stable manifold.

It will become clear in the following that three qualitatively different regimes are detected by varying R, namely:

(a) $R > 1$, where the x axis is unstable to transverse perturbations, so that, being fully unstable, it cannot contribute to the scaling properties of the spectrum of the Schrödinger operator [apart from the fixed point $F1$, which always belongs to the stable manifold because of another special feature of map (1.1): the whole y axis is mapped, in one iterate, onto the point $(2, 0)$, and then onto $F1$].

(b) $1/2 < R < 1$, where all the periodic orbits of the logistic map, to which map (2.4) reduces for $y = 0$, are stable to transverse perturbations (except for $F1$), and a nontrivial recurrent set is present outside the x axis.

(c) $0 < R < 1/2$, where also $F1$ becomes a saddle point, whereas the recurrent set outside the x axis reduces to the fully unstable fixed point $F3$.

3.1. The Structure of the Stable Manifold

In order to describe the recurrent set, we first identify a region L_0 which we prove to escape to infinity, and then we determine its preimages (whenever they exist). For the sake of clarity, it is useful to identify the region L_0 through the union of the two partially overlapping subregions (see Fig. 1)

$$L_1 \equiv \{(x_0, y_0) \mid x_0 < -2,\ y_0 > 0\}$$

$$L_2 \equiv \{(x_0, y_0) \mid x_0 < -1/R,\ y_0 > (1 - R)\, x_0 + 2R\}$$

These sets were already studied in ref. 12. To be self-contained, it is useful to rephrase the results contained in Lemmas 3 and 5 of ref. 12 in our notations.

Proposition 1. Any point in $L_0 = L_1 \cup L_2$ is asymptotically mapped to infinity by (2.4).

Proof. In order to prove that any point in L_1 is mapped to infinity, it is convenient to introduce the variable $a_k \equiv x_k/2$ and rewrite the recursion (2.4), by eliminating y_k,

$$a_{k+1} = 1 - 2a_k^2 - 2Ra_k(a_k - 1 + 2a_{k-1}^2) \tag{3.4}$$

By imposing the inequalities

$$a_{k-1} < -1, \qquad a_k < -a_{k-1}^2 \tag{3.5}$$

one obtains from Eq. (3.4)

$$a_k < -1, \qquad a_{k+1} < -a_k^2$$

This shows, by induction, that $a_k \to -\infty$ for $k \to +\infty$. From the definition of L_1, $a_1 < 1 - 2a_0^2$ and $a_0 < -1$, so that conditions (3.5) are fulfilled already for $k = 1$, and the first part of the proposition is proved.

The proof that any point in L_2 escapes to infinity is analogous. By introducing the variable $b_k = -Rx_k$ one can rewrite Eq. (2.4) in the form

$$b_{k+1} = b_k^2 + 2R(b_k - 1) + b_k(b_k - b_{k-1}^2)/R \tag{3.6}$$

If the conditions

$$b_k > 1, \qquad b_k > b_{k-1}^2$$

are satisfied, then, from Eq. (3.6),

$$b_{k+1} > 1, \qquad b_{k+1} > b_k^2 \tag{3.7}$$

Once again this proves by induction that $b_k \to +\infty$ for $k \to +\infty$, the region L_2 corresponding to the set where conditions (3.7) are fulfilled for $k = 0$. Q.E.D.

Our estimate of the escaping region can be widened by iterating backward the border of L_0, and retaining the $x < 0$ branch only. By repeating indefinitely this procedure, we enlarge L_0 up to reach a region L delimited by an invariant curve. Since the fixed points $F1$ and $F3$ belong to the border of L, it is compelling to conjecture that such an invariant curve is composed of invariant manifolds of the two fixed points. More precisely, accurate numerical calculations (based on a standard series expansion) indicate that the asymptotic invariant curve is composed of (i) the stable manifold of the upper fixed point and the lowest branch of the unstable manifold of the lower fixed point for $R < 1$; and (ii) the stable manifold of $F3$ and the half straight line ($y = 0$, $x < -2$) for $R > 1$. This is because, for

$R > 1$, the region L is limited from below by the straight line $y = 0$, which is an invariant manifold of the dynamics. As a consequence, the asymptotic preimage of such a line coincides with itself, thus defining the border of the escaping region. It is important to observe that, for any $R > 0$, the stable manifold of the upper fixed point reaches the lower fixed point. The reason is that the latter is stable under the action of inverse map (3.1).

Because of the symmetry existing between the preimages of map (2.4), all points in region $D \equiv \{(x, y) \mid (-x, -y) \in L\}$ escape to infinity as well. In particular, by applying the operator S to the border of L, we obtain the border ∂D of D (see Fig. 2). Now, by further determining the whole cascade of all preimages of D (whenever they exist), we generate an infinite family of escaping regions. Starting from the region D itself, we note that only the subset bounded from above by the straight line $y = R(2 - x)$ is invertible. By iterating backward this sector, which touches the x axis in the point $(2, 0)$, we expect to find—from the invariance of the x axis—two distinct regions still touching such an axis in two symmetric points. Because of the special nature of $(2, 0)$, the two points coincide with the center of symmetry (the origin), and moreover, the whole y axis, entirely mapped onto $(2, 0)$, contributes to define the border. As a result, the two backward images of D identify a new escaping region S_1 delimited by the straight line $x = 0$ and by $(\partial D)^{-1}$ (where we denote by C^{-i} the ith preimage of a curve C).

We can now apply the same procedure to the invertible subset of S_1. At variance with the previous case, a single preimage defines *per se* a sector (namely, $S_2^{(1)}$ and $S_2^{(2)}$). The reason is that the intersection of S_1 with the x axis (the origin) has now two distinct preimages). One of the two borders of $S_2^{(i)}$ $(i = 1, 2)$ is simply obtained by taking the preimage of the y axis,

$$y = x - \frac{2}{x} \tag{3.8}$$

It is again independent of R, but its further preimages no longer exhibit this property.

Each sector can be again iterated backward giving rise to two new sectors, all of them intercepting the x axis in preimages of suitable order of the maximum of the logistic map, namely in $\pm(2 \pm (2 \pm \cdots)^{1/2})^{1/2}$. As a result, a sequence of nonoverlapping sectors $S_m^{(i)}$ is obtained. It seems reasonable to conjecture that they exhaust all the regions which escape to infinity, so that their union represents the complement to the stable manifold of the strange repeller.

A careful numerical check of this hypothesis has been performed by means of a direct numerical simulation of the repeller structure. Following

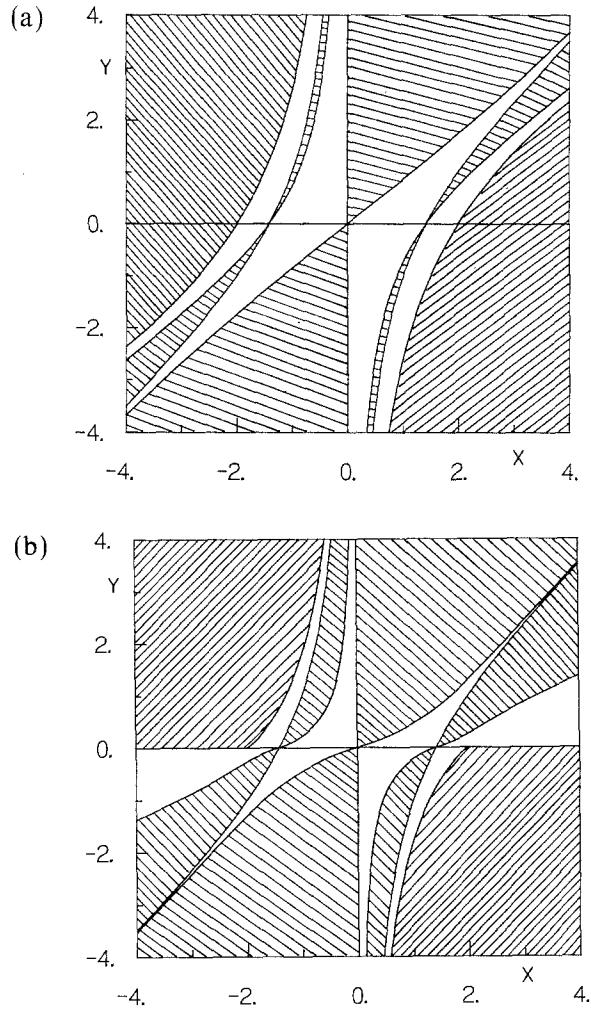

Fig. 2. Preimages of the escaping region L for $R = 0.7$ (a) and 1.5 (b) (shaded).

ref. 18, we start with a generic segment, transverse to the stable manifold of the repeller. By varying the initial condition on the segment, we determine a point P_0 lying within a distance $\delta_{\min}$ from the stable manifold. This is done by checking whether the images of P_0 remain inside a finite region at least for a number $n = \log \delta_{\min}/\lambda_+$ of iterates (where λ_+ is the positive Lyapunov exponent). Then, the point P_0 is iterated until its distance from the stable manifold becomes larger than a preassigned accuracy $\delta_{\max}$.

When this is the case, the accuracy is again increased by repeating the initial procedure. The outcome of a simulation performed over 10^4 iterates is presented in Fig. 3. We observe a Cantor-like structure in correspondence to the sectors identified by our previous approach, thus confirming that the complement to the union of all sectors coincides with the stable manifold of the repeller.

3.2. The Structure of the Unstable Manifold

The investigation of the structure of the unstable manifold is more complex, due to the noninvertibility of map (2.4). However, we can first prove that some regions cannot belong to the repeller. Let us observe that, by direct inspection of Eqs. (3.1), the (x, y) plane can be partitioned into three regions separated by the two parallel straight lines (i) $y = R(2-x)$, (ii) $y = -R(2+x)$:

$$\begin{aligned} C_1 &= (x, y \mid y < -R(2+x)) \\ C_2 &= (x, y \mid -R(2+x) < y < R(2-x)) \\ C_3 &= (x, y \mid y > R(2-x)) \end{aligned} \tag{3.9}$$

All points in C_3 have no preimage in the real plane, as already shown at the beginning of this section. It is also straightforward to observe that all

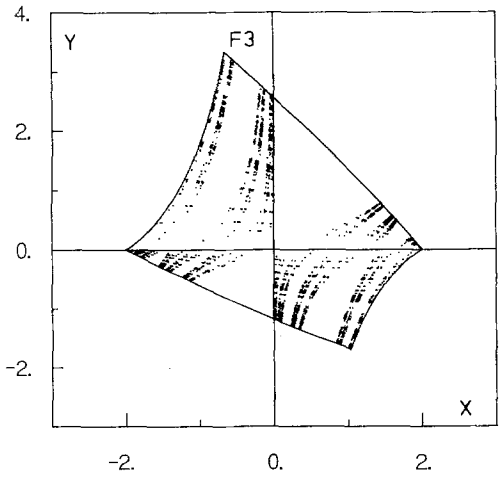

Fig. 3. Direct numerical simulation of the repeller for $R = 1.5$, with its contour as determined from the invariant manifold of $F3$.

points in C_2 have both their preimages in C_2, while the region C_1 is simultaneously mapped backward onto the sector $A=(x, y \mid x<-2, y<0)$, which is a subset of C_1 itself, and onto its symmetric $S(A)$ lying inside C_3.

We can prove the following result.

Lemma 1. The sector A is attracted by the negative x component of map (3.1) toward the fixed point $F1$, for $R>1/2$.

Proof. First, recall that $F1$ is a fully stable fixed point of (3.1) for $R>1/2$. Let us consider the square $\diamond_q=(x, y \mid -2-q<x<-2, -q<y<0)\subset A$. Its preimage in C_1 lies into a closed region Ω bounded by the four following curvilinear segments:

$$\text{(i)} \quad y=0, \quad -(4-q)^{1/2}<x<-2$$

$$\text{(ii)} \quad y=x-\frac{4+q}{x}, \quad -\left[4+\frac{q}{R}(1+R)\right]^{1/2}<x<-(4+q)^{1/2}$$

$$\text{(iii)} \quad y=\frac{q}{Rx}, \quad -\left[4+\frac{q}{R}(1+R)\right]^{1/2}<x<-\left(4+\frac{q}{R}\right)^{1/2}$$

$$\text{(iv)} \quad y=x-\frac{4}{x}, \quad -\left(4+\frac{q}{R}\right)^{1/2}<x<-2$$

Note that all these are monotonic functions in A. As a consequence, the region Ω is contained in a new square $\diamond_{q'}$ whose side length is

$$q'=\max\left\{F(q)=\left[4+\frac{q}{R}(1+R)-2\right]^{1/2}, G(q)=\frac{q}{R(4+q/R)^{1/2}}\right\} \tag{3.10}$$

The stable fixed point of (3.10) is $q=0$ for $R>1/2$, i.e., any square sector in A is eventually mapped backward to $F1$. Q.E.D.

For $R<1/2$ the mapping (3.10) has the stable fixed point $q^*=1/R-4R$, i.e., any square sector A with side length $q>q^*$ contracts into the square sector $\diamond_{q^*}$, which contains $F3$. This implies that $\diamond_{q^*}$ contains a finite portion of L_2. It is reasonable to conjecture that the segment $(x=-1/R,\ 0<y<(2R^2+R-1)/R)$ will be mapped backward in C_1 by (3.1) to the invariant curve joining $F1$ with $F3$. The two lower vertices of $\diamond_{q^*}$ can be proved to be mapped in $F3$. As a consequence, $\diamond_{q^*}$ will contract to the invariant line joining $F1$ to $F3$. Therefore, if no periodic orbit exists on this invariant curve, the sector A of Lemma 1 contracts to $F3$ for $R<1/2$.

We are now in the position to prove the following.

Theorem. The points in region $\Gamma \equiv (\gamma \cap C_2)$, with γ being the concave region outside the parabola

$$y + R^2 = \frac{1}{4}\left(y\frac{1+R}{R} + Rx \right)^2 \tag{3.11}$$

are mapped by (3.1) for $R > 1/2$ either to the fixed point $F1$ or in C_3, where they can no longer be iterated. Thus, all the points in Γ except $F1$ do not belong to the repeller.

Proof. By construction, all points in Γ are mapped backward either in a subset of C_1 or in C_3 [since parabola (3.11) is the image of the two straight lines delimiting C_1 and C_3]. The preimages of points in C_1, in turn, belong to the sector A and to C_3. Then, from Lemma 1, all points in A are attracted by $F1$, while their symmetric preimages lie in C_3. Q.E.D.

According to the comments following Lemma 1, an analogous result should hold also for $R < 1/2$, replacing $F1$ with $F3$, although we have not proved it.

As the repeller is, by definition, an invariant set, it must be located in C_2 inside the convex region delimited by parabola (3.11) (see Fig. 4). This region can be further refined according to the following reasoning. So far, we have excluded those points whose two preimages are attracted by $F1$,

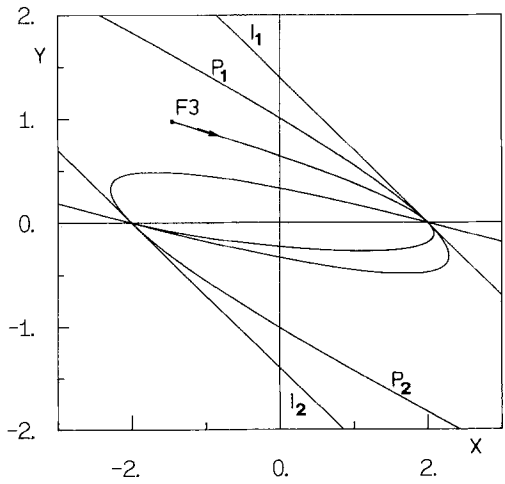

Fig. 4. Escaping regions under the inverse map (3.1) for $R = 0.7$. The two parallel straight lines I_1 and I_2 allow one to identify the regions C_1, C_2, and C_3 defined by Eq. (3.9). Parabola P_1 is the preimage of I_1, I_2, while P_2 is its symmetric under transformation (3.3). The remaining curve represents the unstable manifold of $F3$.

and lie in C_3, respectively. Now, we can add those points whose two preimages are attracted by $F1$. To do that, we must first introduce the parabola symmetric to (3.11), under transformation (3.3). The points belonging simultaneously to the concave regions outside both parabolas (see Fig. 4) fulfill the above requests. As a consequence, by iterating forward the upper part of parabola (3.11), we obtain a refinement of the region containing the repeller. It is now obvious that the procedure can be repeated, by iterating the upper part of the curve which delimits the region. Asymptotically, we expect a convergence toward an invariant manifold. This is confirmed by numerical calculations (see Figs. 1, 3, and 4), which suggest that such an invariant manifold is nothing but a part of the unstable manifold of the fixed point $F3$.

Summarizing these results, we can say that the nontrivial part of the repeller is confined inside a finite region Σ_0 delimited, for $R>1$, by the lower branch of the stable manifold of $F3$ (connecting $F3$ to $F1$) and by the branch of the unstable manifold of $F3$ which connects again $F3$ to $F1$, passing through $(2, 0)$. In fact, this region is also delimited by the symmetric under (3.3) of the stable manifold of $F3$ (see Fig. 3). Since for $R=1/2$, $F1$ coincides with $F3$, such a region disappears and it is therefore natural to conjecture that the recurrent set outside the x axis reduces to the fixed point $F3$ for $0<R<1/2$.

For $R>2$ the region Σ_0 containing the repeller is further restricted by a new mechanism originated by a qualitative change of the unstable manifold of $F1$. For $R>1$, the existence of points of the repeller arbitrarily close to the x axis depends on the dynamical evolution close to $F1$. In fact, the x axis is fully unstable, and the only points reinjected close to it are those falling close to the y axis. More precisely, the segment delimited by the points $(0, y')$ and $(\delta, \bar{y})$ (with $\delta \ll 1$) is iterated in two steps onto the segment having one extremum in $F1$ and angular coefficient $\beta = -R^2/(2+R)$, independent of y' and $\bar{y}$. The multipliers of map (2.4) at $F1$ are 4 and $2R$, the corresponding eigenvectors being $(1, 0)$ and $(1, 2-R)$.[3,5] Since $\beta<2-R$, such a segment lies below the unstable manifold T of $F1$ transverse to the x axis. The points of the repeller lying closer to the x axis are necessarily obtained by iterating forward the points of the above segment. As long as a linear analysis applies, the forward images remain below T, since the second multiplier is larger than 0. Therefore, all the points belonging to the region τ delimited by the first closed loop of T around $(0, 0)$ do not belong to the repeller (see Fig. 5). Moreover, as T is more expanding than the other unstable manifold, points of the repeller infinitesimally close to $F1$ come arbitrarily near T. Accordingly, T represents a border of the repeller, which is thus contained in $\Sigma_1 = \Sigma_0 \backslash \tau$.

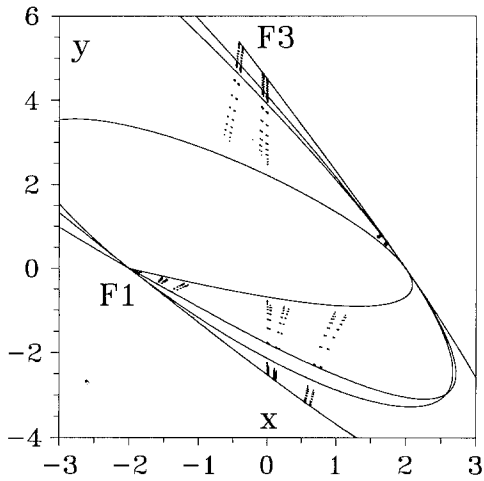

Fig. 5. Unstable manifolds of the fixed points $F1$ and $F3$ for $R = 2.4$ together with the repeller obtained by direct numerical simulation.

Further refinements of the bounds of the repeller are obtained by forward iteration of Σ_1, which is made of two bands lying on opposite sides of the x axis (see Fig. 5). The iteration of each band gives rise to two new bands lying respectively above and below the x axis. If the union of the four bands contains Σ_1, no more gaps are opened and the repeller is continuous along the stable manifold. Otherwise two cases are given:

(a) The four bands do not overlap [apart from F_1 and $(2, 0)$] and a perfectly binary Cantor structure is generated along the stable manifold. One can in fact easily prove that no new overlaps are created at the following steps. The dynamics on the repeller is completely invertible, although the map is globally noninvertible.

(b) The four bands partly overlap, thus leading to a more intricate Cantor-like structure along the stable manifold.

In Fig. 5 we show an example of case (b) for $R = 2.4$, when only one of the two gaps which could be opened at the next hierarchical step is in fact present. Case (a) occurs for larger values of R, while for $R > 2$ we never observe continuity along the stable manifold.

Below $R = 2$ the x axis is the most expanding manifold of $F1$ and the reinjected points come arbitrarily close to it. Therefore the region τ vanishes and there is no mechanism able to generate a fractal structure along the stable manifold. For $1 < R < 2$ the repeller, being continuous and Cantor along the stable and unstable manifold, respectively, has the

topological structure of a typical strange attractor iterated backward in time.

A detailed analysis of the skeleton of the repeller based on the identification of the periodic orbits of (2.4) will be presented in Part II.[16]

Another way of controlling the structure of the repeller close to the x axis is by estimating the fractal dimension D_f along the stable manifold near the x axis. Following the same reasoning that led us to characterize the reinjection mechanism around $F1$, we first observe that a point at a distance δ from the y axis is mapped at a distance δ from $F1$. To detect the singular structure close to the x axis one has to iterate further this point until its distance from $F1$ is $\mathcal{O}(1)$. From the knowledge of the multipliers at $F1$, one derives that the number of required iterates is

$$n = -\frac{\log \delta}{\log 4} \tag{3.12}$$

The corresponding distance ε from the x axis is related to δ by

$$\frac{\log \varepsilon}{\log \delta} = \frac{\log(2/R)}{\log 4} \tag{3.13}$$

The scaling behavior close to the y axis given by the typical square-root law at the band edge $p = \delta^{1/2}$, where p is the measure of points within a distance δ from the y axis. Therefore, from Eq. (3.13) we have

$$D_f = \frac{\log p}{\log \varepsilon} = \frac{\log 2}{\log(2/R)} \tag{3.14}$$

For $R \to 2_-$, $D_f \to \infty$, in agreement with the previous findings that the repeller does not reach the x axis for $R > 2$. For $1 < R < 2$, $D_f > 1$, implying a low density near the x axis as shown in Fig. 3. Finally, for $R < 1$, $D_f < 1$, implying a concentration of points around the x axis. This latter fact is a consequence of the stability of the x axis with respect to transverse perturbations.

4. DYNAMICAL VERSUS SPECTRAL PROPERTIES

In ref. 12 it was proved that the spectrum of model (2.1) is purely singular continuous for $R \geqslant 1$, while for $R < 1$ it is continuous, apart from the possible existence of a pointlike component associated with unbounded sequences $\{x_n\}$ satisfying the conditions

$$x_n < -\frac{1}{R}, \qquad x_n > -Rx_{n-1}^2, \qquad \forall n \geqslant n_0 \tag{4.1}$$

with x_n monotonously approaching $-\infty$ and n_0 any fixed integer. In ref. 12 no conclusion was reached about the existence of this component of the spectrum. In this section we discuss this problem by analyzing Eqs. (2.4) and (3.1). Let us first observe that conditions (4.1) define a region Π in the (x, y) plane bounded by the curves

$$B_1: \quad y = (1-R)x - \frac{2}{x} \tag{4.2}$$

$$B_2: \quad y = x - \frac{2R+1}{Rx} \tag{4.3}$$

Our aim is to identify a region Π_∞ in the (x, y) plane such that $\{x_n\}$ diverges monotonously to $-\infty$, remaining inside Π for each $n \geqslant 1$ (where it is convenient to choose $n_0 = 1$, without any loss of generality). In fact, once such a region is found, it is sufficient to take all its preimages to obtain all the orbits which satisfy inequalities (4.1). By definition, this region is the intersection of all the preimages of Π according to (3.1),

$$\Pi_\infty = \bigcap_{i=0}^{\infty} \Pi_i \tag{4.4}$$

where Π_i is the ith preimage of Π. We address here the question of whether Π_∞ is empty or not.

As a preliminary, let us prove the following.

Lemma 2. The left preimage according to map (3.1) of any curve

$$y = \alpha x + f(x) \tag{4.5}$$

with $f(x) \to 0$ when $x \to -\infty$ converges to

$$y = (1-R)x + \bar{f}(x) \tag{4.6}$$

where $\bar{f}(x)$ has the same asymptotic property of $f(x)$.

Proof. From the inverse mapping (3.1), one obtains that the left preimage of $y = \alpha x + f(x)$ is given by the curve

$$y = \alpha' x + f'(x)$$

where $f'(x) \to 0$ for $x \to -\infty$, and

$$\alpha' = \frac{\alpha}{\alpha + R}$$

This recursive relation has a stable fixed point in $\alpha = \alpha^* = (1 - R)$. Therefore any curve of the form (4.5), restricted to the invertibility region defined in (3.2), converges to a curve of the same form with an asymptote of slope α^*, and the Lemma is proved. Q.E.D.

Let us observe now that both B_1 and B_2 belong to the family of curves (4.5) and, moreover, they intersect each other in the fixed point $F3$. It is natural to distinguish between two cases:

$$\text{(i)} \quad 0 < R < 1/2, \qquad \text{(ii)} \quad 1/2 \leqslant R < 1$$

Case (i). $F3$ is fully unstable and no other fixed point of (2.4) lies inside Π. Local stability analysis shows that the most unstable eigendirection of $F3$ points inside Π. Combining this observation with Lemma 2, one deduces that the preimages of both B_1 and B_2 converge to the branch of the unstable manifold of $F3$ contained inside Π and, reasonably, this convergence is monotonous. As a consequence, one can state the following:

Conjecture 1. Π_∞ coincides with the union of the branch of the unstable manifold of $F3$ contained inside Π and its symmetric under transformation (3.3).

This symmetric curve has to be included, because it, too, is a preimage of the manifold (so, technically, it belongs to the invariant manifold). However, no further points have to be added, as it has no preimage, lying in the noninvertibility region defined by (3.2).

In order to relate this result to the spectral properties of the associated Schrödinger tight-binding problem, one has to identify the intersections of Π_∞ with the set of initial conditions $y = \lambda$, $x = E - 2$. This implies that for any fixed positive λ, the pointlike component of the spectrum exists if and only if λ is larger than the opposite of the y coordinate of $F3$, that is,

$$\lambda > \frac{1}{R} - 1 - 2R \tag{4.7}$$

and it corresponds to the highest excited state of the spectrum.

Case (ii). The region Π now contains also the fully unstable fixed point $F1$, while $F3$ is a saddle (see Fig. 1b). In this case the preimages of B_1 and B_2 tend monotonously to the branch of the unstable manifold of $F1$ which diverges to $-\infty$ and to the branch of the stable manifold of $F3$ joining this fixed point with $F1$. On the other hand, the sequences $\{x_n\}$ that may eventually diverge to $-\infty$ according to (4.1) are those whose initial condition onto lies the unstable branch of $F1$ fully contained inside Π. Therefore one can put forward the following:

Conjecture 2. Π_∞ coincides with the union of the branch of the unstable manifold of $F1$ contained inside Π and its symmetric under (3.3).

At variance with case (i), now the pointlike component located at the highest excited state of the spectrum is present for any positive λ.

Let us stress that the results of this section on the existence of a pointlike component in the spectrum rely on the conjectures. Their

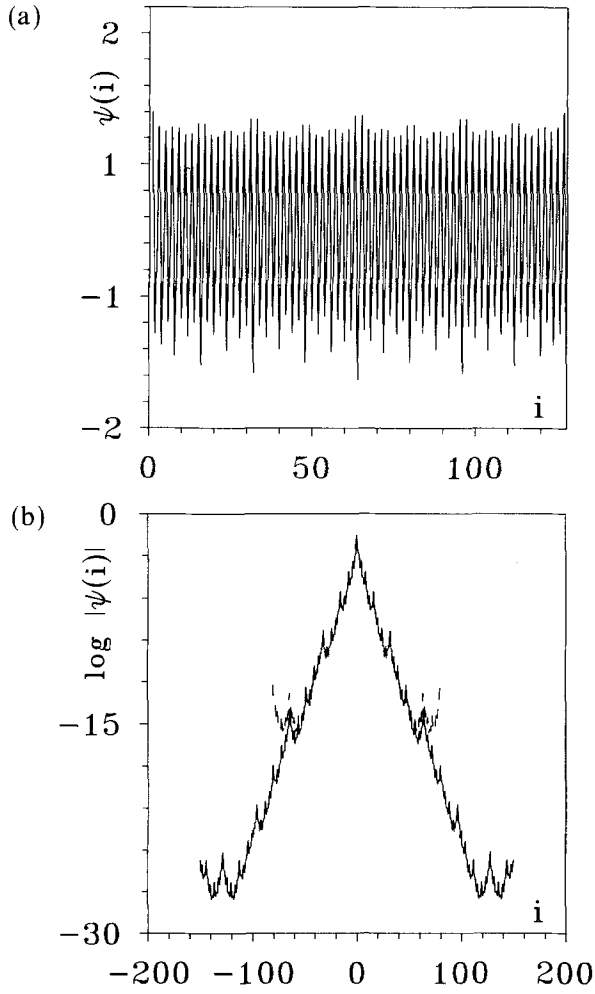

Fig. 6. Wavefunctions of the Schrödinger operator (2.1) of the most excited state, for $R=0.3$. (a) The periodic approximation of hierarchical order $n=7$; (b) the results for $n=7$ (dashed curve) and $n=8$ (solid curve) are compared, by shifting the peak of the wavefunction to the same site $n=0$.

correctness depends in turn on the monotonous convergence to Π_∞. Let us also observe that the relation between the pointlike component and a suitable part of the unstable manifold allows for a direct location of this spectral component.

To have a confirmation of our conclusions, we have evaluated the wavefunction of the Schrödinger operator (1.1) for different periodic approximations. More precisely, by exploiting the renormalization transformations (see also ref. 5) we have first determined the energy of the rightmost band edge of a generic order i of hierarchical approximation. The further substitution in Eq. (2.1) allowed us to determine the initial conditions $\psi(1)$, $\psi(2)$ such that $\psi(2^n+1)=\psi(1)$, $\psi(2^n+2)=\psi(2)$, and the wavefunction is normalized.

In Fig. 6 we report the results for $R=0.3$ and two λ values, 1 and 2.5, below and above the critical value $\lambda_c=26/15$ [as from Eq. (4.7)], respectively. In the first case the wavefunction is clearly an extended oscillating state. In the second case, the plot of the logarithm of the absolute value of ψ indicates an exponential localization. The peak coincides with the position of the highest barrier $i=2^n$. To compare the curves resulting from two different approximations (namely $n=7$ and 8), we displaced the peaks to the same site $n=0$. The extremely good agreement between the two curves around the maximum indicates that the result is already asymptotic. A numerical fit of the slope gives a localization length $l_c \simeq 5$.

6. CONCLUSIONS AND PERSPECTIVES

We have studied the structure of the chaotic repeller of map (2.4) by identifying regions of the (x, y) plane which escape to infinity. Complementary information has been obtained by analyzing the structure of the invariant manifolds. Both methods allow the determination of the minimal region containing the repeller, which turns out to be fractal along the unstable manifold. The structure along the stable manifold depends on R; we were able to prove its continuity for $R<2$, while for $R>2$ more intricate Cantor-like structures are present.

Moreover, the analysis of the renormalization map with tools of dynamical system theory leads to the derivation of interesting results concerning the associated spectral problem. For instance, we have been able to give a positive answer to the question left open in ref. 12 about the existence of a pointlike component in the spectrum of the hierarchical model studied in this paper. We have also confirmed the conjecture raised in ref. 12 about the location of such a component, providing a direct recipe for its determination. Another peculiarity of this model is the coexistence of localized and extended wavefunctions in different parts of the spectrum for

fixed values of the parameters R and λ. Recently, it has been proven that unbounded, rapidly growing potentials yield localized spectra.[19] Our potential satisfies the conditions of the theorems proved in ref. 19 for $R > 1$. This means that the existence of a singular continuous spectrum is peculiar of Dirichlet boundary conditions and that a more generic initial condition *á la* Kotani leads to a point spectrum. It would be nice to have some results on the stability with respect to initial conditions also for the $R < 1$ case, using the methods of ref. 19.

The contents of this paper almost exhaust the discussion on the topological aspects associated with this hierarchical problem. Further information can be extracted from the knowledge of periodic orbits, whose determination allows one in principle to solve the problem of the scaling properties of the spectrum. The second part of this work[16] will be entirely devoted to the problems of the invariant measure and of multifractal scaling.

ACKNOWLEDGMENTS

We acknowledge useful discussions with J. Bellisard, H. Kunz, R. Lima, L. Pastur, M. Rasetti, and A. Sütó.

REFERENCES

1. M. Kohmoto, L. P. Kadanoff, and C. Tang, *Phys. Rev. Lett.* **50**:1870 (1983).
2. S. Ostlund, R. Pandit, D. Rand, H. J. Schellnhuber, and E. D. Siggia, *Phys. Rev. Lett.* **50**:1873 (1983).
3. T. Schneider, D. Wurtz, A. Politi, and M. Zannetti, *Phys. Rev. B* **36**:1789 (1987).
4. H. E. Roman, *Phys. Rev. B* **36**:7173 (1987).
5. R. Livi, A. Maritan, and S. Ruffo, *J. Stat. Phys.* **52**:595 (1988).
6. D. Würtz, T. Schneider, A. Politi, and M. Zannetti, *Phys. Rev. B* **39**:7829 (1989).
7. B. A. Huberman and M. Kerszberg, *J. Phys. A* **18**:L331 (1985).
8. S. Teitel and E. Domany, *Phys. Rev. Lett.* **55**:2176 (1986).
9. A. Maritan and A. Stella, *J. Phys. A* **19**:L269 (1986).
10. M. Casdagli, *Commun. Math. Phys.* **107**:292 (1986).
11. A. Sütó, *Commun. Math. Phys.* **111**:409 (1987).
12. H. Kunz, R. Livi, and A. Sütó, *Commun. Math. Phys.* **122**:643 (1989).
13. A. Sütó, *J. Stat. Phys.*, to appear.
14. T. Schneider, A. Politi, and D. Würtz, *Z. Phys. B* **66**:469 (1987).
15. H. A. Ceccato, W. P. Keirstead, and B. A. Huberman, *Phys. Rev. A* **36**:5509 (1987).
16. R. Livi, A. Politi, and S. Ruffo, Repeller structure in a hierarchical model. II. Metric properties, *J. Stat. Phys.* **65**:73 (1991).
17. N. Widom, D. Bensimon, L. P. Kadanoff, and S. J. Shenker, *J. Stat. Phys.* **32**:443 (1983).
18. G. H. Hsu, E. Ott, and C. Grebogi, *Phys. Lett. A* **127**:199 (1988).
19. K. Kirsch, S. Molchanov, and L. A. Pastur, Pure point spectrum for 1-d Schrödinger operator with an unbounded potential, preprint Kharkov (1990).